

## Research Article

# Mathematical Modeling and Analysis of COVID-19 Infection: Application to the Kingdom of Saudi Arabia Data

Ebraheem Alzahrani <sup>1</sup> and Muhammad Altaf Khan <sup>2</sup>

<sup>1</sup>Department of Mathematics, Faculty of Science, King Abdulaziz University, P.O. Box 80203, Jeddah 21589, Saudi Arabia

<sup>2</sup>Institute for Ground Water Studies, Faculty of Natural and Agricultural Sciences, University of the Free State, Bloemfontein, South Africa

Correspondence should be addressed to Muhammad Altaf Khan; [altafdir@gmail.com](mailto:altafdir@gmail.com)

Received 17 May 2023; Revised 20 July 2023; Accepted 5 November 2023; Published 14 November 2023

Academic Editor: Yusuf Pandir

Copyright © 2023 Ebraheem Alzahrani and Muhammad Altaf Khan. This is an open access article distributed under the Creative Commons Attribution License, which permits unrestricted use, distribution, and reproduction in any medium, provided the original work is properly cited.

To evaluate the probable effects of the COVID-19 outbreak on Saudi Arabia, a novel dynamical model is developed. Using the most recent instances of COVID-19 infection that have been reported in Saudi Arabia, we examine the roles of quarantine and hospitalization. The model's mathematical outcomes are displayed. The model's infection-free equilibrium is displayed, and asymptotically, it is determined to be both locally and globally stable. We demonstrate that the model is locally asymptotically stable (LAS) for the basic reproduction  $\mathcal{R}_0 < 1$ . The model is globally asymptotically stable (GAS) when  $\mathcal{R}_0 \leq 1$ . To estimate the model parameters, recent COVID-19 instances in KSA that began between May 1, 2022, and August 4, 2022, are taken into account. We achieve the needed data fitting considering the approach of nonlinear least square, and we demonstrate that the predicted basic reproduction number is  $\mathcal{R}_0 \approx 1.2988$ . Graphical representations of the calculated parameters and their effects on disease eradication are provided. The findings show that the most effective way to reduce the number of new instances of infection is to limit the contact of exposed, asymptomatic, symptomatic, and hospitalized people with vulnerable. The percentage of exposed people who are quarantined also plays a big part in lowering the number of infected cases.

## 1. Introduction

It is believed in epidemiology that mathematical models are essential for comprehending the dynamics and predicting the long-term behaviors of the sickness. Mathematical models are regarded as the main tools for studying the forecasts and eradication of disease outbreaks with the introduction of new infectious illnesses. Due to coronavirus infection, a huge number of death and infection cases were reported worldwide, while many nations in the world experienced financial crisis [1]. With COVID-19, mainly the low-income countries are badly suffered [2]. The coronavirus effect on the Saudi Arabia's gross domestic product (GDP) can be seen in [3]. Records indicate that a significant number of infected cases in Saudi Arabia ended in death. There have been 9271 fatalities and 812093 total cases documented in the Kingdom to date. The recommendations

of the World Health Organization (WHO) were successfully implemented by the Saudi government and as a result, the infected cases were found decreasing significantly, which is less prevalent than the earlier layers or waves of illness [4]. The outbreak of the coronavirus infection has been recorded in many countries of the world, where many of them experienced with more consecutive layers. In Saudi Arabia, there have been previously three waves of infection cases observed, and now, the fourth wave also occurred with a number of infections and deaths. The previous layers recorded more cases of infection and deaths compared to the recent layer.

A variety of mathematical models have been presented in science and engineering to understand the complicated nonlinear process of physical and biological problems [5–7]. A particular application of the modeling to engineering problems can be seen here [8–10]. For the application of

mathematical modeling to smart phone and image processing, we refer the readers to visit [11–13]. To learn more about mathematical models used to research infectious illnesses, and in particular to comprehend the COVID-19's dynamics, visit [14–23]. For instance, the work in [14] has included the lockdown in modeling coronavirus infection. The authors defined new fractal-fractional operators, and their application to coronavirus has been discussed. The researchers suggested from their results that how individuals can be saved with lockdown when there is no vaccination. In [15], a continuous Markov chain model of coronavirus infection is demonstrated. The authors studied the results for the herd immunity and presented results for the disease forecast. The Omicron variant and its mathematical modeling have been suggested in [16]. The authors used the homotopy perturbation method (HPM) and obtained the analytical and approximate solution for the COVID-19 model. The coronavirus infection and its mathematical modeling using the reported cases have been discussed in [17]. The variable order fractional differential equation and its application to COVID-19 have been used and obtained the theoretical results. Using various control measures to curtail the coronavirus infection has been considered in [18]. The authors considered the real data of eight countries and presented the results. In [19], the mathematical analysis to show the infected cases in Ethiopia has been described. They determined the model parameters and computed the threshold quantity. Also, they provided graphical results for possible elimination of the disease in Ethiopia. The mathematical model is designed to incorporate the stress and tension assumptions in the study given in [20]. In [24], the authors considered a fractional model to study COVID-19 with the impact of vaccination. The concept of quarantine together with the asymptomatic individuals in the formulation of COVID-19 has been studied in [25]. The fractional order using the concept of Mittag-Leffler kernel has been considered to investigate COVID-19 with real data in [26]. The COVID-19 disease with the age study has been formulated and discussed in [27]. They analyzed the stability of the model, obtained sensitivity analysis, and provided some simulation results regarding the disease elimination. A mathematical model to understand the infection cases' trends in KSA has been suggested in [21]. Controlling the outbreak of coronavirus infection, the authors in [28] formulated a fractional model with vaccination. They discussed the role of vaccination in the control of the disease in the society. A numerical study has been organized to solve numerically the COVID-19 system using the Hermite wavelets [29]. The formulation of the coronavirus model in delay differential equations using the fractional order derivative has been discussed in [30]. A study has been organized on coronavirus using the face masks application in [31]. The authors used the real data and studied the impact of the face masks' efficacy and their uses to control the infection. It has been suggested that with the face masks' efficacy and their continuous use during the pandemic, the number of potential cases will decrease effectively. The authors used the compartmental model to estimate the parameters using the KSA data and presented the results.

The authors explored the coronavirus infection under self-isolation study in [22]. They computed the threshold quantity for the proposed model and presented results for the infection elimination. The researchers in [23] constructed a mathematical model under the early reported cases of coronavirus in KSA. They obtained the numerical value of the threshold and found that the infection can be decreased faster when following the recommendation of the WHO. They studied the local and global dynamics of their proposed model and provided the most sensitive parameters that can increase or decrease the threshold quantity. The anxiety causes during the COVID-19 outbreak to people has been studied in [32], the bifurcation analysis involved in the fractional system in [33], and medical imaging in [34]. Some more applications can be seen in [35, 36].

From the coronavirus literature, we highlight here further research output. The scientists took into account a mathematical model for the instances that were recorded in India and produced the best control strategy for any potential disease eradication [37]. The use of face masks is one of the best controls for COVID-19 infection, according to the research published in [38]. Infection with COVID-19 and cholera has both been documented in [39]. Using a mathematical model from [40], specific applications are applied to Turkish data. Coronavirus with decline in immunity has been considered in [41]. The authors in [42] proposed a mathematical model for coronavirus infection and obtained results regarding the infection elimination. A clinical study-based model about the coinfection of dengue and COVID-19 has been explored in [43]. The diffusion process involved in the coronavirus model has been modeled, and the link between the two has been demonstrated in [44]. A delay differential equations model is suggested in [45] to investigate the COVID-19 disease. Some more work that recently studied the coronavirus and other epidemic diseases through nonlinear differential equations are as follows: a mathematical model to study COVID-19 with the crowding effect has been analyzed in [46]. The authors in [47] used the concept of diffusion to analyze the coronavirus infection. Mathematical modeling of the Nipah virus and analysis using the new numerical scheme has been shown in [48]. The impact of treatment on gonorrhoea has been discussed in [49]. Mathematical modeling of Lassa fever in terms of stochastic modeling has been shown in [50]. The dynamics of cancer disease through virotherapy under a new numerical scheme has been considered in [51]. The COVID-19 infection and their control in India have been given in [52], where the authors suggested control strategies for the minimization of the infection. The efficacy of preventive and optimal control analysis for the COVID-19 infection in India has been considered by the authors in [53].

The primary goal of this research is to examine the COVID-19 disease's dynamics in light of a recent report on cases in Saudi Arabia between May 1 and August 4, 2022. The contact of healthy people with exposed, asymptomatic, symptomatic, and hospitalized people is the four transmission channels that are responsible for the disease spread of coronavirus infection in the population. Such force of infection has not yet been considered in the literature to analyze the COVID-19 infection dynamics with real data.

The potential transmission paths for COVID-19 are addressed and pertinent references are given. We developed the model and acquired the requisite mathematical and simulation findings based on these transmissions.

The manuscript will be divided into the following sections: a thorough literature review on COVID-19 and other outcomes of the mathematical modeling have been presented in Section 1. The remaining findings are presented in the following sections. The formulations of the problem are described in Section 2. The model’s mathematical analysis and the stability findings are presented in Sections 3 and 4, respectively. The estimate of the parameters and their numerical outcomes are presented in Section 5. The final findings are presented in Section 6.

## 2. Model Formulation

This part investigates the development of a mathematical model for the dynamics of the SARS-CoV-2 illness under isolation and quarantine. We consider the model of total human population denoted by  $M(t)$  and divide it further into susceptible  $S(t)$  (individuals that can contract the disease), exposed  $E(t)$  (individuals that attracted the disease and undergoes the disease incubation period), asymptomatic  $A(t)$  (individuals that do not show disease symptoms of COVID-19), symptomatic  $I(t)$  (individuals that show disease symptoms of COVID-19), quarantined  $Q(t)$  (individuals that are quarantined during the exposed period), hospitalized individuals  $H(t)$  (individuals that show clinical symptoms and quarantined individuals which are infected and being hospitalized), and recovered individuals  $R(t)$  (individuals in different compartments that are recovered from COVID-19 infection). So, we write the total population as  $M(t) = S(t) + E(t) + A(t) + I(t) + Q(t) + H(t) + R(t)$ , and the force of the infection term is shown by

$$\lambda(t) = \frac{\xi_1 E + \xi_2 A + \xi_3 I + \xi_4 H}{M}, \tag{1}$$

where the healthy individuals after getting in close contact with the exposed, asymptomatic, symptomatic, and hospitalized individuals are infected with the contact rates given by  $\xi_1, \xi_2, \xi_3,$  and  $\xi_4,$  respectively. The contact between healthy and those hospitalized is shown by  $\xi_4,$  as in many countries of the world with fewer medical facilities [54]. The healthy individuals and their contact with the exposed individuals are possible because the virus can easily transfer to healthy individuals through coughing, shaking hands, flu, etc., and this fact has been documented in the literature, see [55–58]. It is well known that individuals in the asymptomatic class have strong immunity and they do not show the disease symptoms until it is tested to be identified or hard to screen for and can easily transmit the infection to healthy people. It has been recorded that most of the COVID-19 cases are from asymptomatic individuals [59, 60]. The interaction of symptomatic people that do not follow the guidelines of COVID-19 and their interaction with vulnerable people increase the number of infections. The hospitalized individuals while facing susceptible individuals

in hospitals and other healthcare centers transmit the infections to healthcare workers. It is recommended that healthcare workers should follow the necessary guidelines, such as using the kits, to reduce the disease’s further spread. The growth rate of the susceptible population is given by the parameter  $\Lambda$ ; as opposed to this,  $\mu$  provides the natural death rate for each compartment in the model. The vulnerable people after getting an infection undergo an incubation period and then split the individual progress into asymptomatic and symptomatic classes, respectively, with the parameters  $\kappa\phi$  and  $(1 - \phi)\kappa$ . The exposed individuals during their exposed period are quarantined at a rate  $\eta_1$ . Individuals who are asymptomatic, symptomatic, quarantined, and hospitalized are shown to recover in turn by the rate  $\gamma_1, \gamma_2, \gamma_3,$  and  $\gamma_4$ . The symptomatic and quarantined people are hospitalized by the rate  $\eta_2$  and  $\eta_3,$  respectively. The parameters  $d_1$  and  $d_2,$  respectively, represent the disease mortality rate of symptomatic and hospitalized individuals. In our model, we do not give a transition from asymptomatic to symptomatic class as there are no visible facts that asymptomatic develops symptoms or it may be later, so we follow the suggestion of [61]. The abovementioned details of the parameters and their compartments are shown in details in Figure 1. The abovementioned brief discussion leads to the development of the evolutionary nonlinear ordinary differential equations given by

$$\begin{cases} \frac{dS}{dt} = \Lambda - \lambda(t)S - \mu S, \\ \frac{dE}{dt} = \lambda(t)S - (\kappa + \mu + \eta_1)E, \\ \frac{dA}{dt} = \kappa\phi E - (\mu + \gamma_1)A, \\ \frac{dI}{dt} = \kappa(1 - \phi)E - (\mu + d_1 + \eta_2 + \gamma_2)I, \\ \frac{dQ}{dt} = \eta_1 E - (\mu + \eta_3 + \gamma_3)Q, \\ \frac{dH}{dt} = \eta_2 I + \eta_3 Q - (\gamma_4 + \mu + d_2)H, \\ \frac{dR}{dt} = \gamma_1 A + \gamma_2 I + \gamma_3 Q + \gamma_4 H - \mu R, \end{cases} \tag{2}$$

with the non-negative initial conditions (ICs)

$$\begin{aligned} S(0) &\geq S_0, E(0) \geq E_0, A(0) \geq A_0, I(0) \geq I_0, \\ Q(0) &\geq Q_0, H(0) \geq H_0, \\ R(0) &\geq R_0. \end{aligned} \tag{3}$$

The following biological feasible region which is positively invariant is considered for the model (2):

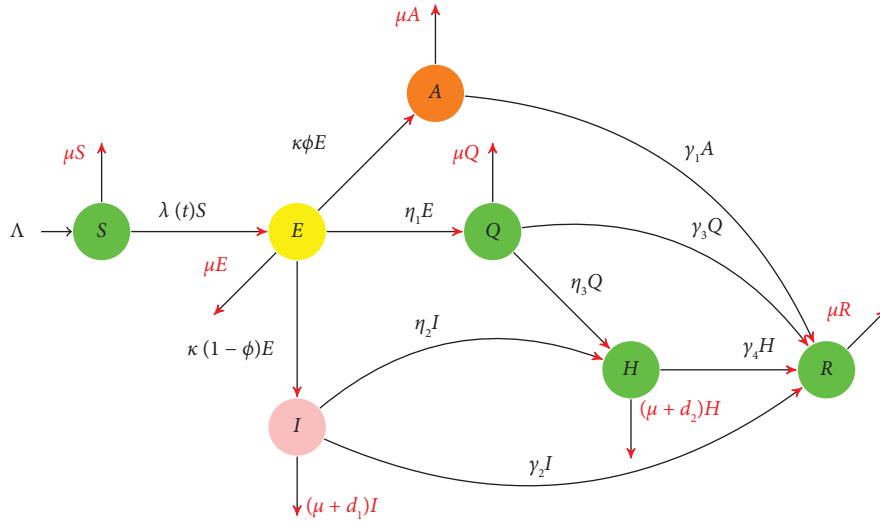


FIGURE 1: The rate of flow of the parameters in system (2).

$$\Gamma = \left\{ (S, E, A, I, Q, H, R) \in \mathbb{R}_+^7 : S, E, A, I, Q, H, R \geq 0, \text{ and } M \leq \frac{\Lambda}{\mu} \right\}, \tag{4}$$

and any system trajectory under an IC shall remain in  $\Gamma$  for each time  $t \geq 0$ . Since the region is positively invariant,  $\Gamma$  may be used to study the dynamical outcomes.

### 3. Mathematical Analysis of the Model

This section studies the mathematical analysis of model (2). For a dynamical system, we first need to determine the possible equilibrium points of model (2). Obviously, two equilibrium points that often involve in the diseases model, such as the disease-free equilibrium (DFE) and the endemic equilibrium (EE). The DFE shall be represented by  $P_0$  of system (2) and can be obtained through the following way:

$$\begin{aligned} P_0 &= (S^0, 0, 0, 0, 0, 0, 0) \\ &= \left( \frac{\Lambda}{\mu}, 0, 0, 0, 0, 0, 0 \right). \end{aligned} \tag{5}$$

**3.1. Basic Reproduction Number.** The basic reproduction number has an important role in disease epidemiology. It characterizes how the disease spread in the population and how it can be controlled. One can easily define the number of average COVID-19 infection cases introduced to the healthy population who have not yet infected and produced a number of new secondary cases. Usually, in the literature, it is commonly denoted by  $\mathcal{R}_0$ . For compartmental models of the disease, the approach of the next-generation matrix is often used to obtain the expression for the basic reproduction number [62]. For the given model (2), with the abovementioned approach, we obtain the required matrices as follows:

$$\begin{aligned} F &= \begin{pmatrix} \xi_1 & \xi_2 & \xi_3 & 0 & \xi_4 \\ 0 & 0 & 0 & 0 & 0 \\ 0 & 0 & 0 & 0 & 0 \\ 0 & 0 & 0 & 0 & 0 \\ 0 & 0 & 0 & 0 & 0 \end{pmatrix}, \\ V &= \begin{pmatrix} (\eta_1 + \kappa + \mu) & 0 & 0 & 0 & 0 \\ -\kappa\phi & (\gamma_1 + \mu) & 0 & 0 & 0 \\ -\kappa(1 - \phi) & 0 & (\gamma_2 + d_1 + \eta_2 + \mu) & 0 & 0 \\ -\eta_1 & 0 & 0 & (\gamma_3 + \eta_3 + \mu) & 0 \\ 0 & 0 & -\eta_2 & -\eta_3 & (\gamma_4 + d_2 + \mu) \end{pmatrix}. \end{aligned} \tag{6}$$

Furthermore, we need to compute the spectral radius of  $\rho(FV^{-1})$  that shall gives the basic reproduction number  $\mathcal{R}_0$  of system (2) given by

$$\begin{aligned} \mathcal{R}_0 = & \frac{\xi_1}{(\eta_1 + \kappa + \mu)} + \frac{\eta_2 \kappa \xi_4 (1 - \phi)}{(\eta_1 + \kappa + \mu)(\gamma_2 + d_1 + \eta_2 + \mu)(\gamma_4 + d_2 + \mu)} \\ & + \frac{\eta_1 \eta_3 \xi_4}{(\eta_1 + \kappa + \mu)(\gamma_3 + \eta_3 + \mu)(\gamma_4 + d_2 + \mu)} + \frac{\kappa \xi_2 \phi}{(\eta_1 + \kappa + \mu)(\gamma_1 + \mu)} \\ & + \frac{\kappa \xi_3 (1 - \phi)}{(\eta_1 + \kappa + \mu)(\gamma_2 + d_1 + \eta_2 + \mu)}. \end{aligned} \tag{7}$$

Here, the expression given by  $\mathcal{R}_1$  accounts for the generation of secondary infection due to the interaction of the exposed individuals with healthy individuals. The expressions  $\mathcal{R}_2$  and  $\mathcal{R}_3$  account for the cases due to hospitalized individuals. The secondary infected cases due to asymptomatic contact are generated through the expression  $\mathcal{R}_4$ . The secondary cases generated by the symptomatic individuals by contacting the healthy people are shown by  $\mathcal{R}_5$ . It should be noted that  $\xi_1 \neq \xi_2 \neq \xi_3 \neq \xi_4$ .

3.2. *Endemic Equilibria.* The endemic equilibrium denoted by  $P_1$  can be determined for model (2) by making the time rate of change equal to zero and is given by

$$\left\{ \begin{aligned} S^* &= \frac{\Lambda}{\lambda^* + \mu}, \\ E^* &= \frac{\lambda^* S^*}{(\eta_1 + \kappa + \mu)}, \\ A^* &= \frac{\kappa \phi E^*}{(\gamma_1 + \mu)}, \\ I^* &= \frac{\kappa (1 - \phi) E^*}{(\gamma_2 + d_1 + \eta_2 + \mu)}, \\ Q^* &= \frac{\eta_1 E^*}{(\gamma_3 + \eta_3 + \mu)}, \\ H^* &= \frac{\eta_3 Q^* + \eta_2 I^*}{(\gamma_4 + d_2 + \mu)}, \\ R^* &= \frac{\gamma_1 A^* + \gamma_3 Q^* + \gamma_4 H^* + \gamma_2 I^*}{\mu}. \end{aligned} \right. \tag{8}$$

Inserting (8) into the force of the infection term gives

$$\lambda^* = \frac{\xi_1 E^* + \xi_2 A^* + \xi_3 I^* + \xi_4 H^*}{M}, \tag{9}$$

and we get the following:

$$z_0 \lambda^* + z_1 = 0, \tag{10}$$

where

$$\begin{aligned} z_0 = & ((\gamma_3 + \eta_3 + \mu)(\eta_2 \kappa (1 - \phi)(\gamma_4 + \mu) \\ & + (\gamma_4 + d_2 + \mu)(\kappa (1 - \phi)(\gamma_2 + \mu) \\ & + \mu(\gamma_2 + d_1 + \eta_2 + \mu))) \\ & \times (\gamma_1 + \mu) + \eta_1 (\gamma_2 + d_1 + \eta_2 + \mu)(\gamma_1 + \mu) \\ & \cdot (\eta_3 (\gamma_4 + \mu) + (\gamma_4 + d_2 + \mu)(\gamma_3 + \mu)) \\ & + \kappa (\gamma_2 + d_1 + \eta_2 + \mu) \\ & \cdot (\gamma_3 + \eta_3 + \mu)(\gamma_4 + d_2 + \mu)\phi(\gamma_1 + \mu), \\ z_1 = & \mu (\eta_1 + \kappa + \mu)(\gamma_1 + \mu) \\ & \cdot (\gamma_2 + d_1 + \eta_2 + \mu)(\gamma_3 + \eta_3 + \mu) \\ & \cdot (\gamma_4 + d_2 + \mu)(1 - \mathcal{R}_0). \end{aligned} \tag{11}$$

We see that  $z_0 > 0$  and  $z_1$  can be positive if  $\mathcal{R}_0 < 1$ . It can be observed from (11) that a positive endemic equilibrium exists only if  $\mathcal{R}_0 > 1$ .

### 4. Stability Analysis

For the disease-free situation, both locally and globally, the stability analysis of model (2) shall be explored in the present section. The following theorems are given.

**Theorem 1.** *The COVID-19 system is LAS if  $\mathcal{R}_0 < 1$  and the Routh–Hurtwitz conditions  $W_1–W_5$  are met.*

*Proof.* We shall compute the Jacobian matrix of system (2) and its evaluation based on the disease-free case  $P_0$ , which is computed and is given by

$$J(P_0) = \begin{pmatrix} -\mu & -\xi_1 & -\xi_2 & -\xi_3 & 0 & -\xi_4 & 0 \\ 0 & m_1 & \xi_2 & \xi_3 & 0 & \xi_4 & 0 \\ 0 & \kappa\phi & -(\gamma_1 + \mu) & 0 & 0 & 0 & 0 \\ 0 & \kappa(1 - \phi) & 0 & -(\gamma_2 + d_1 + \eta_2 + \mu) & 0 & 0 & 0 \\ 0 & \eta_1 & 0 & 0 & -(\gamma_3 + \eta_3 + \mu) & 0 & 0 \\ 0 & 0 & 0 & \eta_2 & \eta_3 & -(\gamma_4 + d_2 + \mu) & 0 \\ 0 & 0 & \gamma_1 & \gamma_2 & \gamma_3 & \gamma_4 & -\mu \end{pmatrix}, \tag{12}$$

where  $m_1 = \xi_1 - (\eta_1 + \kappa + \mu)$ . We have two roots for  $J(P_0)$  that contains negative real parts  $\lambda_{1,2} = -\mu$ , while the rest of the five eigenvalues can be determined through the following equations:

$$\lambda^5 + k_1\lambda^4 + k_2\lambda^3 + k_3\lambda^2 + k_4\lambda + k_5 = 0, \tag{13}$$

where

$$\begin{aligned} k_1 &= \gamma_1 + \gamma_2 + \gamma_3 + \gamma_4 + d_1 + d_2 + \eta_2 + \eta_3 + 4\mu + (\eta_1 + \kappa + \mu)(1 - \mathcal{R}_1), \\ k_2 &= (\gamma_4 + d_2 + \mu)(\gamma_2 + d_1 + \eta_2 + \mu) + (\gamma_3 + \eta_3 + \mu)(\gamma_2 + d_1 + \eta_2 + \mu) \\ &\quad + (\gamma_3 + \eta_3 + \mu)(\gamma_4 + d_2 + \mu) + (\gamma_1 + \mu)(\gamma_2 + \gamma_3 + \gamma_4 + d_1 + d_2 + \eta_2 + \eta_3 + 3\mu) \\ &\quad + (\gamma_1 + \mu)(\eta_1 + \kappa + \mu)(1 - \mathcal{R}_1 - \mathcal{R}_4) + (\eta_1 + \kappa + \mu)(\gamma_2 + d_1 + \eta_2 + \mu)(1 - \mathcal{R}_1 - \mathcal{R}_5) \\ &\quad + (\eta_1 + \kappa + \mu)(\gamma_3 + \gamma_4 + d_2 + \eta_3 + 2\mu)(1 - \mathcal{R}_1), \\ k_3 &= (\gamma_1 + \mu)((\gamma_3 + \eta_3 + \mu)(\gamma_4 + d_2 + \mu) + (\gamma_2 + d_1 + \eta_2 + \mu)(\gamma_3 + \gamma_4 + d_2 + \eta_3 + 2\mu)) \\ &\quad + (\gamma_3 + \eta_3 + \mu)(\eta_1 + \kappa + \mu)(\gamma_2 + d_1 + \eta_2 + \mu)(1 - \mathcal{R}_1 - \mathcal{R}_5) \\ &\quad + (\gamma_3 + \eta_3 + \mu)(\gamma_4 + d_2 + \mu)(\gamma_2 + d_1 + \eta_2 + \mu) + (\gamma_3 + \eta_3 + \mu)(\gamma_4 + d_2 + \mu) \\ &\quad \times (\eta_1 + \kappa + \mu)(1 - \mathcal{R}_1 - \mathcal{R}_3) + (\gamma_1 + \mu)(\gamma_3 + \eta_3 + \mu)(\eta_1 + \kappa + \mu)(1 - \mathcal{R}_1 - \mathcal{R}_4) \\ &\quad + (\gamma_4 + d_2 + \mu)(\eta_1 + \kappa + \mu)(\gamma_2 + d_1 + \eta_2 + \mu)(1 - \mathcal{R}_1 - \mathcal{R}_2 - \mathcal{R}_5) \\ &\quad + (\gamma_1 + \mu)(\eta_1 + \kappa + \mu)(\gamma_2 + d_1 + \eta_2 + \mu)(1 - \mathcal{R}_1 - \mathcal{R}_4 - \mathcal{R}_5) \\ &\quad + (\gamma_1 + \mu)(\gamma_4 + d_2 + \mu)(\eta_1 + \kappa + \mu)(1 - \mathcal{R}_1 - \mathcal{R}_4), \\ k_4 &= (\gamma_1 + \mu)(\gamma_3 + \eta_3 + \mu)(\gamma_2 + d_1 + \eta_2 + \mu)(\gamma_4 + d_2 + \eta_1 + \kappa + 2\mu) \\ &\quad + (\gamma_3 + \eta_3 + \mu)(\gamma_4 + d_2 + \mu)(\eta_1 + \kappa + \mu)(\gamma_2 + d_1 + \eta_2 + \mu)(1 - \mathcal{R}_1 - \mathcal{R}_2 - \mathcal{R}_3 - \mathcal{R}_5) \\ &\quad + (\gamma_1 + \mu)(\gamma_3 + \eta_3 + \mu)(\eta_1 + \kappa + \mu)(\gamma_2 + d_1 + \eta_2 + \mu)(1 - \mathcal{R}_1 - \mathcal{R}_4 - \mathcal{R}_5) \\ &\quad + (\gamma_1 + \mu)(\gamma_3 + \eta_3 + \mu)(\gamma_4 + d_2 + \mu)(\eta_1 + \kappa + \mu)(1 - \mathcal{R}_1 - \mathcal{R}_3 - \mathcal{R}_4) \\ &\quad \cdot (\gamma_1 + \mu)(\gamma_4 + d_2 + \mu)(\eta_1 + \kappa + \mu)(\gamma_2 + d_1 + \eta_2 + \mu)(1 - \mathcal{R}_1 - \mathcal{R}_2 - \mathcal{R}_4 - \mathcal{R}_5), \\ k_5 &= (\gamma_1 + \mu)(\gamma_3 + \eta_3 + \mu)(\gamma_4 + d_2 + \mu)(\eta_1 + \kappa + \mu)(\gamma_2 + d_1 + \eta_2 + \mu)(1 - \mathcal{R}_0). \end{aligned} \tag{14}$$

It can be observed from the coefficients of equation (13) that all  $k_j$  for  $j = 1, \dots, 5$  are positive depending on the value

of  $\mathcal{R}_0$  less than 1. Furthermore, one can establish the Routh–Hurtwitz criteria given by

$$\begin{aligned} W_1 &= k_1, W_2 = \begin{pmatrix} k_1 & 1 \\ k_3 & k_2 \end{pmatrix}, W_3 = \begin{pmatrix} k_1 & 1 & 0 \\ k_3 & k_2 & k_1 \\ 0 & 0 & k_3 \end{pmatrix}, \\ W_4 &= \begin{pmatrix} k_1 & 1 & 0 & 0 \\ k_3 & k_2 & k_1 & 0 \\ 0 & k_4 & k_3 & k_2 \\ 0 & 0 & 0 & k_4 \end{pmatrix}, W_5 = \begin{pmatrix} k_1 & 1 & 0 & 0 & 0 \\ k_3 & k_2 & k_1 & 1 & 0 \\ k_5 & k_4 & k_3 & k_2 & k_1 \\ 0 & 0 & k_5 & k_4 & k_3 \\ 0 & 0 & 0 & 0 & k_5 \end{pmatrix}, \end{aligned} \tag{15}$$

to ensure that equation (13) contains all eigenvalues with negative real parts. So, we can conclude that the infection-free equilibrium of model (2) is locally asymptotically stable provided that  $\mathcal{R}_0 < 1$ .

Next, we give the global stability of the infection-free equilibrium.  $\square$

**Theorem 2.** *If  $\mathcal{R}_0 \leq 1$ , then at the infection-free state  $P_0$ , system (2) is GAS.*

*Proof.* We obtain the global stability results by defining the Lyapunov function and is given by

$$\mathcal{L}(t) = w_1E(t) + w_2A(t) + w_3I(t) + w_4Q(t) + w_5H(t). \tag{16}$$

Here,  $w_1, \dots, w_5$  are constants and positive, and their numerical value in later stepping of the proof shall be obtained. Now inserting system (2) into (16) and simplifying, we get

$$\begin{aligned} \mathcal{L}'(t) &= w_1[\lambda S - (\kappa + \mu + \eta_1)E] + w_2[\kappa\phi E - (\mu + \gamma_1)A] + w_3[\kappa(1 - \phi)E - (\mu + d_1 + \eta_2 + \gamma_2)I] \\ &\quad + w_4[\eta_1E - (\mu + \eta_3 + \gamma_3)Q] + w_5[\eta_2I + \eta_3Q - (\gamma_4 + \mu + d_2)H] \\ &= \left[ w_1\xi_1\frac{S}{M} + w_4\eta_1 + w_2\kappa\phi + w_3\kappa(1 - \phi) - (\kappa + \mu + \eta_1)w_1 \right] E + \left[ w_1\xi_2\frac{S}{M} - w_2(\mu + \gamma_1) \right] A \\ &\quad + \left[ w_1\xi_3\frac{S}{M} - w_3(\mu + d_1 + \eta_2 + \gamma_2) + \eta_2w_5 \right] I + [w_5\eta_3 - w_4(\mu + \eta_3 + \gamma_3)]Q \\ &\quad + \left[ w_1\xi_4\frac{S}{M} - w_5(\gamma_4 + \mu + d_2) \right] H \\ &\leq [w_1\xi_1 + w_4\eta_1 + w_2\kappa\phi + w_3\kappa(1 - \phi) - (\kappa + \mu + \eta_1)w_1]E + [w_1\xi_2 - w_2(\mu + \gamma_1)]A \\ &\quad + [w_1\xi_3 - w_3(\mu + d_1 + \eta_2 + \gamma_2) + \eta_2w_5]I + [w_5\eta_3 - w_4(\mu + \eta_3 + \gamma_3)]Q \\ &\quad + [w_1\xi_4 - w_5(\gamma_4 + \mu + d_2)]H. \end{aligned} \tag{17}$$

In the last step of (17), we used  $S/M \leq 1$ . Furthermore, considering the value of the constants  $w_1 = (\mu + d_1 + \eta_2 + \gamma_2)(\mu + d_2 + \gamma_4)$ ,  $w_2 = (\mu + d_1 + \eta_2 + \gamma_2)(\mu + d_2 + \gamma_4)\xi_2$ ,  $w_3 = (\xi_4\eta_2 + \xi_3(\gamma_4 + \mu + d_2))$ ,  $w_4 = \eta_3\xi_4(\mu + d_1 + \eta_2 + \gamma_2)/(\mu + \eta_3 + \gamma_3)$ , and  $w_5 = \xi_4(\mu + d_1 + \eta_2 + \gamma_2)$  in (17), we get

$$\mathcal{L}'(t) \leq (\kappa + \mu + \eta_1)(\mu + d_1 + \eta_2 + \gamma_2) \cdot (\mu + d_2 + \gamma_4)(\mathcal{R}_0 - 1)E. \tag{18}$$

Here, if  $\mathcal{R}_0 \leq 1$ , then  $\mathcal{L}'(t) \leq 0$  and if  $E = 0$ , then  $\mathcal{L}'(t) = 0$ . So, system (2) at the infection-free state  $P_0$  is globally asymptotically stable on  $\Gamma$  provided that  $\mathcal{R}_0 \leq 1$ .  $\square$

## 5. Parameters Estimations and Numerical Simulation

**5.1. Parameters Estimations.** Here, we focus on the most recent instances of COVID-19 recorded in Saudi Arabia between May 1 and August 4, 2022; for more information, visit [4]. The actual cases are obtained from Worldometer on daily bases. According to the data details given in [4], it is the fourth wave in the country, which has fewer cases as compared to the other three waves in the country. We used the data of the given period and apply the curve fitting technique and desired results are obtained in time units per day. In this curve fitting analysis, we consider the birth by estimating

from the data while the natural death rate has been obtained from the literature. The total population of Saudi Arabia in 2022 has been considered to be  $M(0) = 35942111$ . The following are the starting conditions used to acquire the data fitting:  $S(0) = 35881882$ ,  $E(0) = 60000$ ,  $A(0) = 100$ ,  $I(0) = 99$ ,  $Q(0) = 10$ ,  $H(0) = 20$ , and  $R(0) = 0$ . The infected cases (symptomatic case)  $I(0) = 99$ , which is the first case of COVID-19 at the beginning of the fourth wave on May 1, 2022. The other initial conditions are subjected to the data fitting. Up until the required desired fitting to the data is attained, the least square curve fitting approach has been used to simulate the data fitting to the model. The results of the data fitting to the model have been shown graphically in Figure 2, whereas the fitted/estimated values of the parameters are given in Tables 1 and 2. Table 2 contains the model parameters fitted to the model with 95% confidence interval (CI). Considering the listed values of the parameters given in Tables 1 and 2, one can estimate the numerical value of the basic reproduction number to be  $\mathcal{R}_0 \approx 1.2988$ . According to the nature of the data, the present fitting is considered to be good and its estimated parameters can be used to further study the behavior of the model and the possible disease elimination. Figure 3 shows the simulation of  $\mathcal{R}_0$  versus the model parameters. It can be seen that increase or decrease in these parameters as a function of  $\mathcal{R}_0$  will increase or decrease the basic reproduction number.

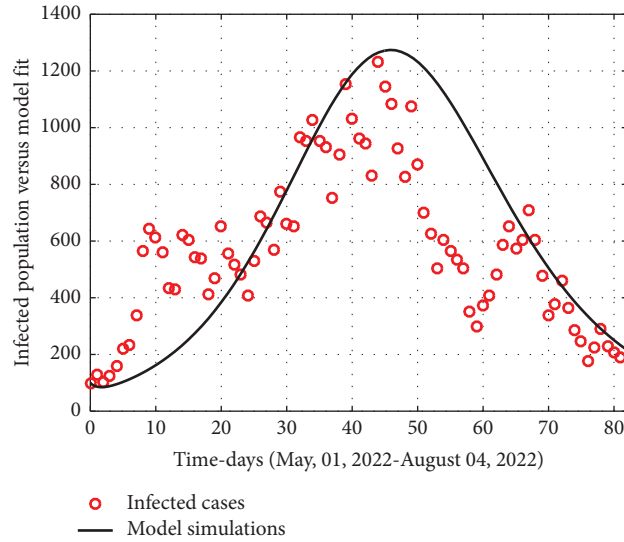


FIGURE 2: The reported new cases of coronavirus in Saudi Arabia and its fitting to the model. The solid line indicates the model solution while the red circles are the cases.

TABLE 1: Estimated parameters and those taken from the literature.

Symbols	Definitions	Numeric values	References
$\Lambda$	Recruitment rate	$d \times M(0)$	Estimated
$\mu$	Natural death rate	$1/74.87 \times 365$	[4]
$d_1$	Disease mortality rate of symptomatic infected	0.015	[63, 64]
$d_2$	Disease mortality rate of hospitalized individuals	0.04	[63, 64]
$\gamma_4$	People recovered from hospitalization	0.1250	[64]
$\eta_1$	Quarantined rate of exposed people	0.1962	[64]
$\eta_2$	Hospitalization rate of symptomatic people	0.0221	[64]

TABLE 2: Parameters estimated for the system with 95% CI.

Symbols	Definitions	95% CI	Base values	References
$\xi_1$	Contact rate due to exposed	[0.3426–0.4477]	0.3952	Fitted
$\xi_2$	Contact rate due to asymptomatic	[0.1539–0.2426]	0.1982	Fitted
$\xi_3$	Contact rate due to symptomatic	[0.0102–0.0155]	0.0128	Fitted
$\xi_4$	Contact rate due to hospitalization	[0.0023–0.0058]	0.004	Fitted
$\kappa$	Incubation period	[0.1211–0.1677]	0.1444	Fitted
$\phi$	Fraction of individuals that do not show symptoms	[0.9915–0.9934]	0.9924	Fitted
$\gamma_1$	People recovered from asymptomatic infection	[0.5662–0.6396]	0.6029	Fitted
$\gamma_2$	People recovered from symptomatic infection	[0.8006–0.8824]	0.8415	Fitted
$\gamma_3$	People recovered from quarantined infection	[0.4228–0.5247]	0.4738	Fitted
$\eta_3$	Hospitalization rate of quarantined people	[0.0101–0.0126]	0.0113	Fitted

5.2. Numerical Simulation. The numerical values listed in Tables 1 and 2 and the initial conditions of the system variables used in the estimations of parameters have been utilized to obtain simulation results of model (2). We obtain the simulation of model (2) using the sensitive parameters, which are beneficial for disease elimination. In Figure 4, we consider the impact of the parameter  $\xi_1$  on the infected population, and it can be observed that minimizing the contact of the healthy individuals with those who have disease symptoms can best decrease the infected cases further in the community. One of the importance of awareness among people is to be isolated and make social

distance from the people who are considered to threat to the spread of the infection.

The impact of the parameter  $\xi_2$  on the infected population is shown in Figure 5. It can be seen that protection from asymptomatic people is critical as it cannot be identified that the individuals are infected unless it is being tested. So, the general guidelines suggested by the World Health Organization (WHO) should be followed strictly to reduce future cases of infection, see Figure 5.

The infected individuals after getting treatment in hospitals can also infect healthcare workers [65–67] and a number of deaths have been reported in the aforementioned references. It



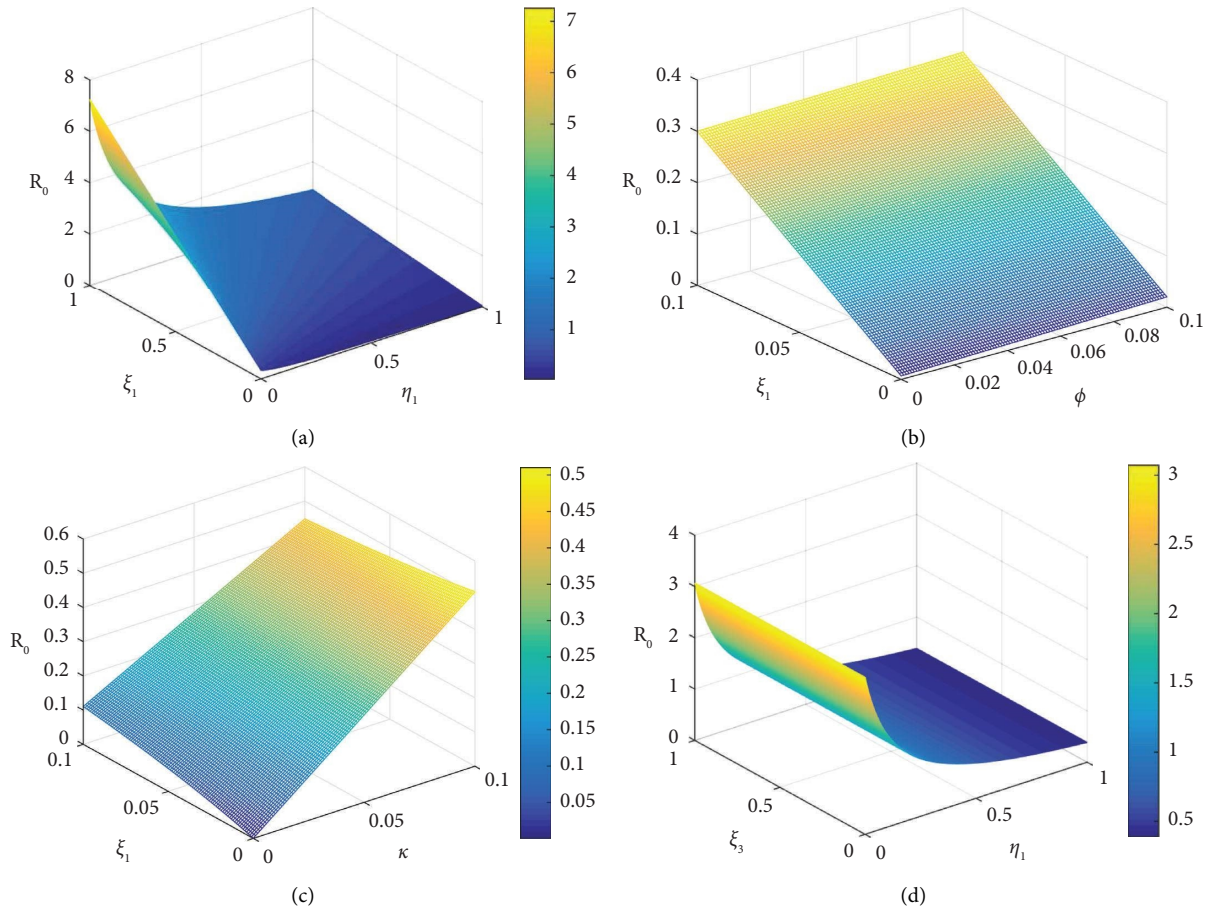


FIGURE 3: The plot shows the simulation of  $\mathcal{R}_0$  as a function of the parameters. 3D subplots: (a)  $\mathcal{R}_0$  as a function of  $\eta_1$  and  $\xi_1$ , (b)  $\mathcal{R}_0$  as a function of  $\phi$  and  $\xi_1$ , (c)  $\mathcal{R}_0$  as a function of  $\xi_1$  and  $\kappa$ , and (d)  $\mathcal{R}_0$  as a function of  $\xi_3$  and  $\eta_1$ .

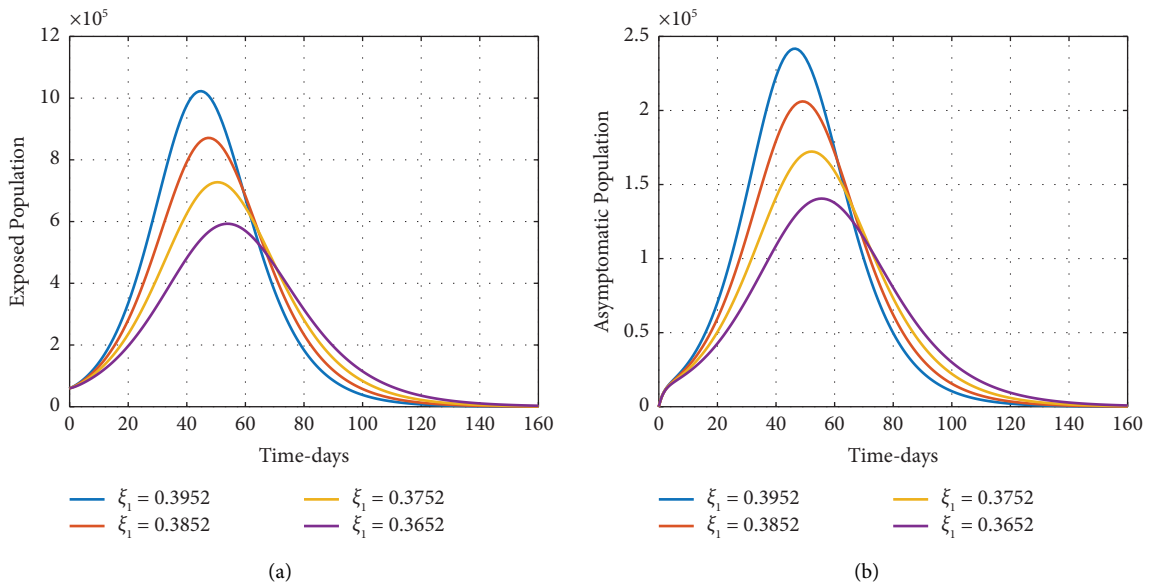


FIGURE 4: Continued.

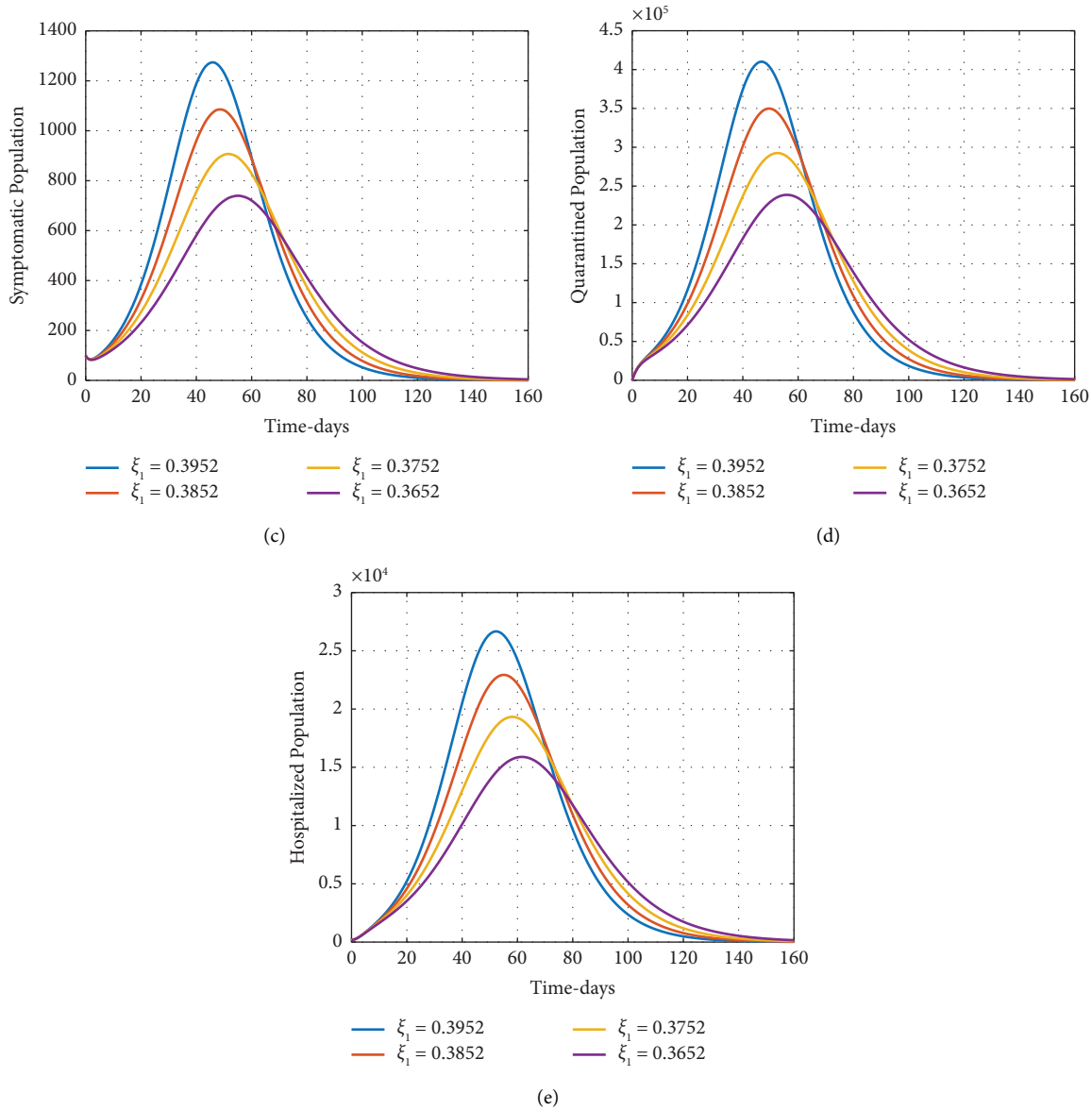


FIGURE 4: The simulation of the infected compartments of system (2) with various values of  $\xi_1$ . Subgraphs (a)–(e), respectively, represent the behavior of compartments  $E$ ,  $A$ ,  $I$ ,  $Q$ , and  $H$ .

is also noted from the literature that a number of medical workers has been infected during treating the infected people in hospitals and some have died. So, the proper guidelines suggested for the healthcare workers must be implemented to reduce the death of the healthcare workers and the future spread of the infection, see Figure 6. It can be observed from Figure 6 that proper guidelines followed by the healthcare workers may decrease well the future infection.

We give Figure 7 to see the impact of the parameter  $\phi$  on the dynamics of the infected compartments of the model. The parameter  $\phi$  is the fraction of individuals; while completing the incubation period, the individuals are separated based on the infection, asymptomatic or symptomatic. The literature suggests that asymptomatic people have great contributions in the disease progress; a high percentage of cases have been reported due to asymptomatic infection.

Therefore, if possible, many individuals should be tested and those identified to be asymptomatic must be isolated to reduce future cases. The parameter value of  $\phi$  is obtained from data fitting and is reasonable to the literature. By lowering this value, it becomes clear from Figure 7 that there are fewer asymptomatic instances while there are more symptomatic cases, which is the result of  $(1 - \phi)$ .

Similarly, decreasing the value of  $\kappa$ , the number of infected cases increases for exposed, quarantined, and hospitalized individuals while decreasing for the asymptomatic and symptomatic people, see Figure 8. The role of quarantine of the exposed individuals has been considered useful in many infectious diseases such as SARS and Ebola and also found useful for SARS-CoV-2 infection. Increasing the number of quarantine individuals will minimize the number of future cases.

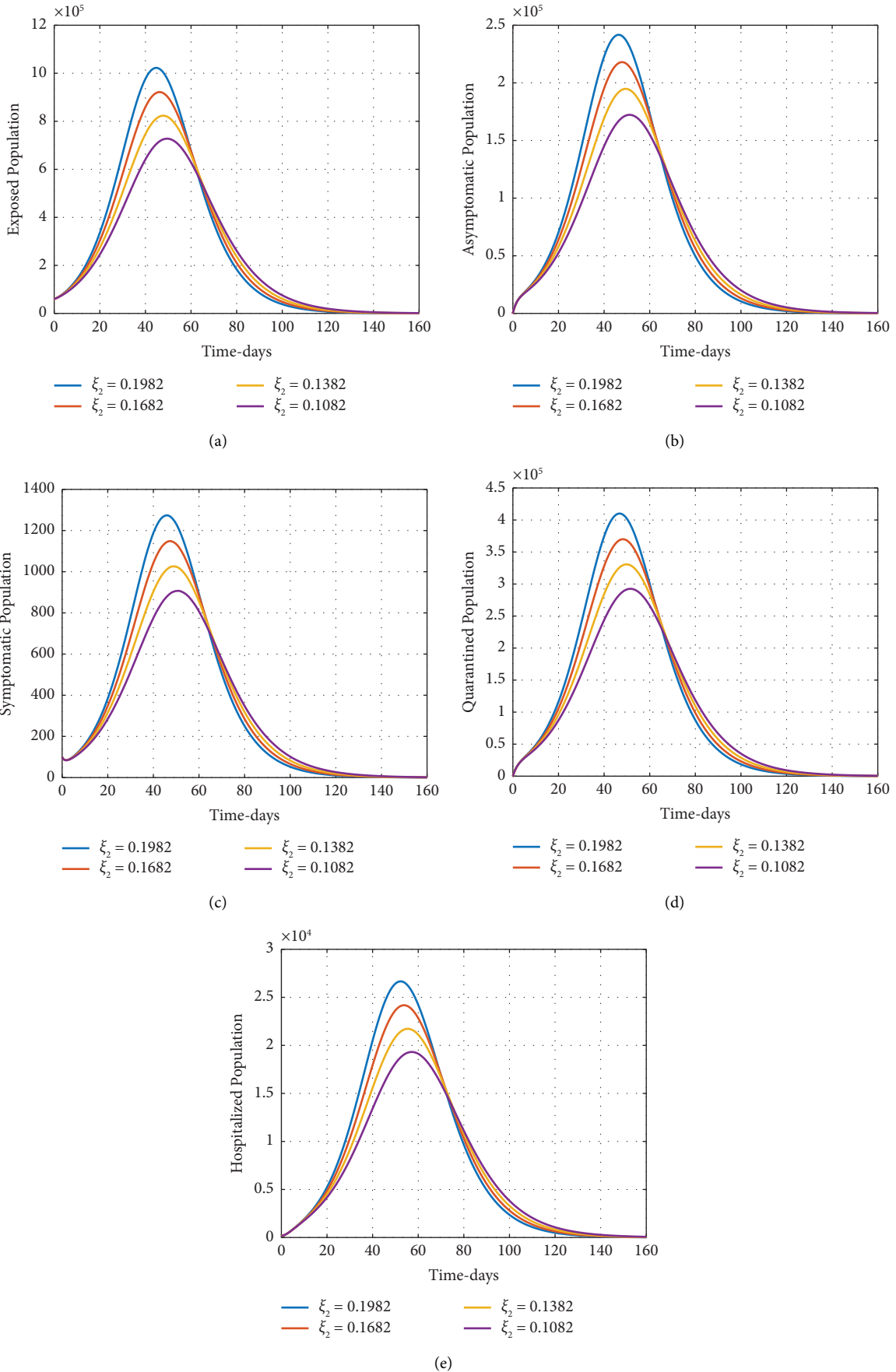
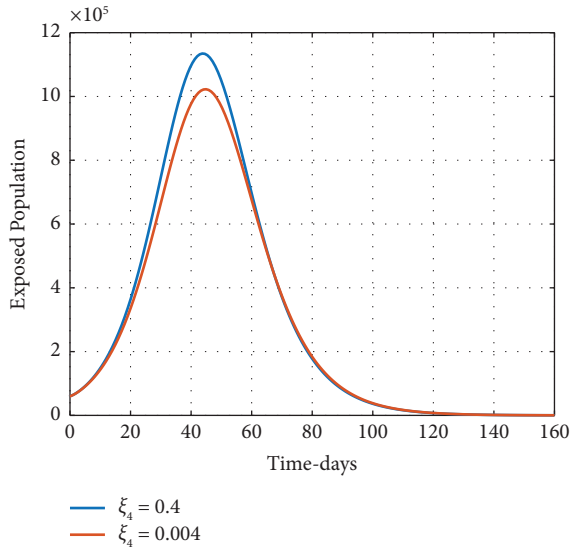
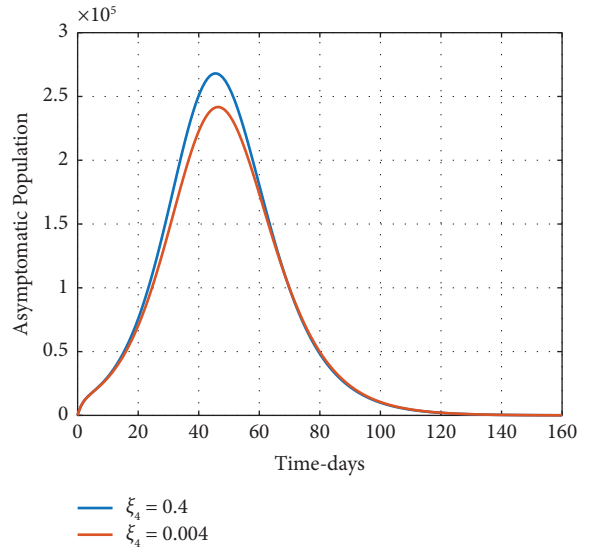


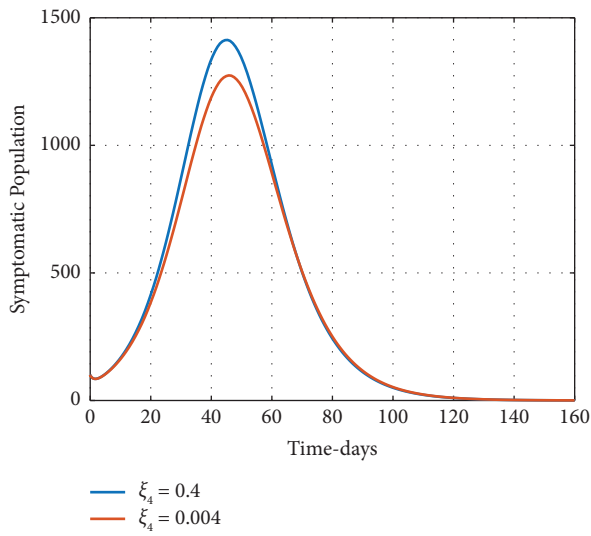
FIGURE 5: The simulation of the infected compartments of system (2) with various values of  $\xi_2$ . Subgraphs (a)–(e), respectively, represent the behavior of compartments  $E$ ,  $A$ ,  $I$ ,  $Q$ , and  $H$ .



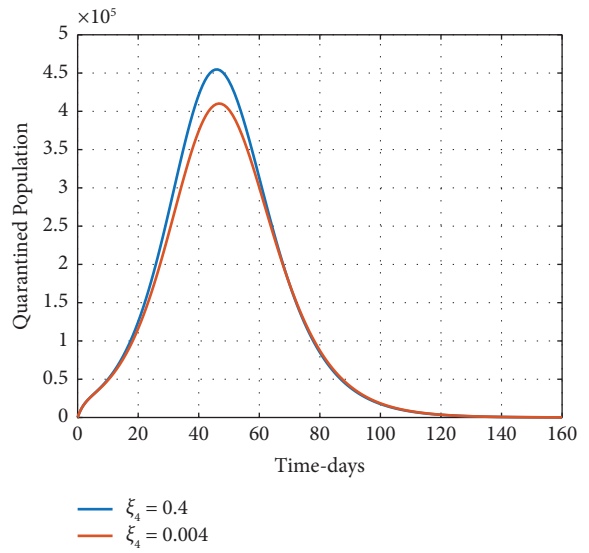
(a)



(b)

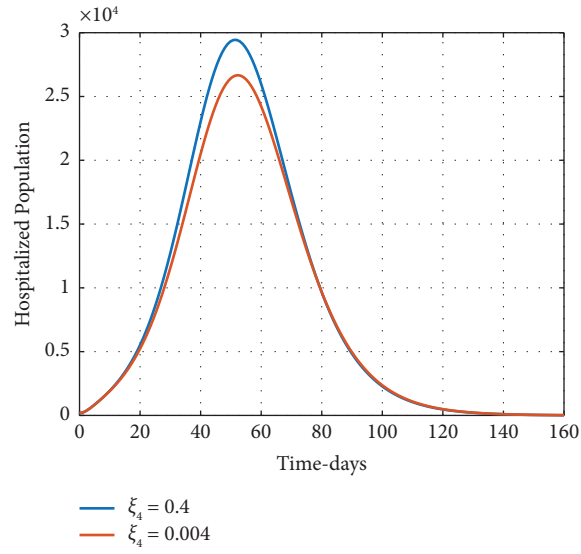


(c)



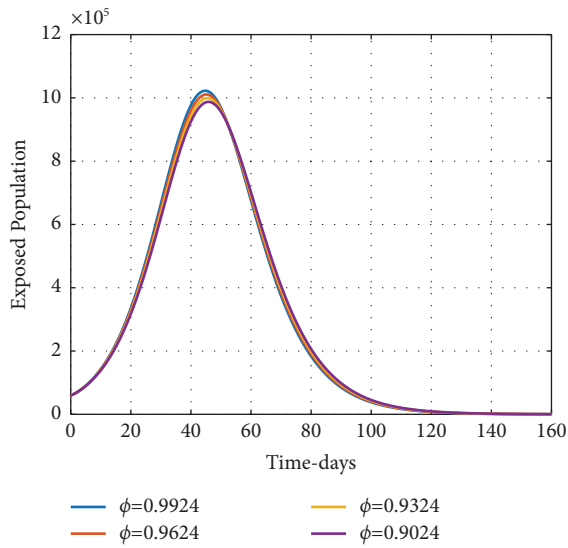
(d)

FIGURE 6: Continued.

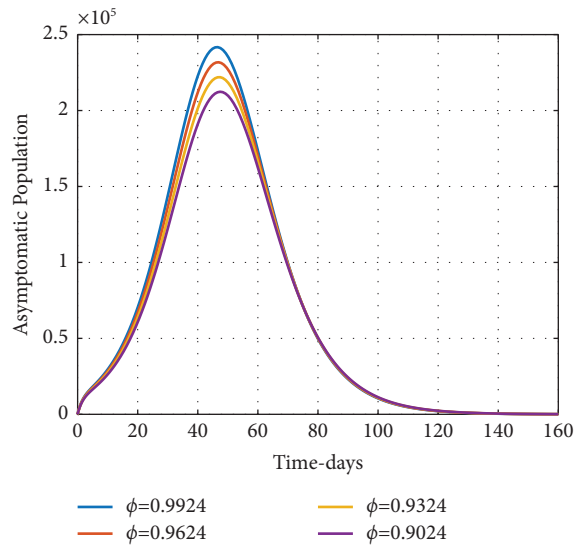


(e)

FIGURE 6: The simulation of the infected compartments of system (2) with various values of  $\xi_3$ . Subgraphs (a)–(e), respectively, represent the behavior of compartments  $E$ ,  $A$ ,  $I$ ,  $Q$ , and  $H$ .



(a)



(b)

FIGURE 7: Continued.

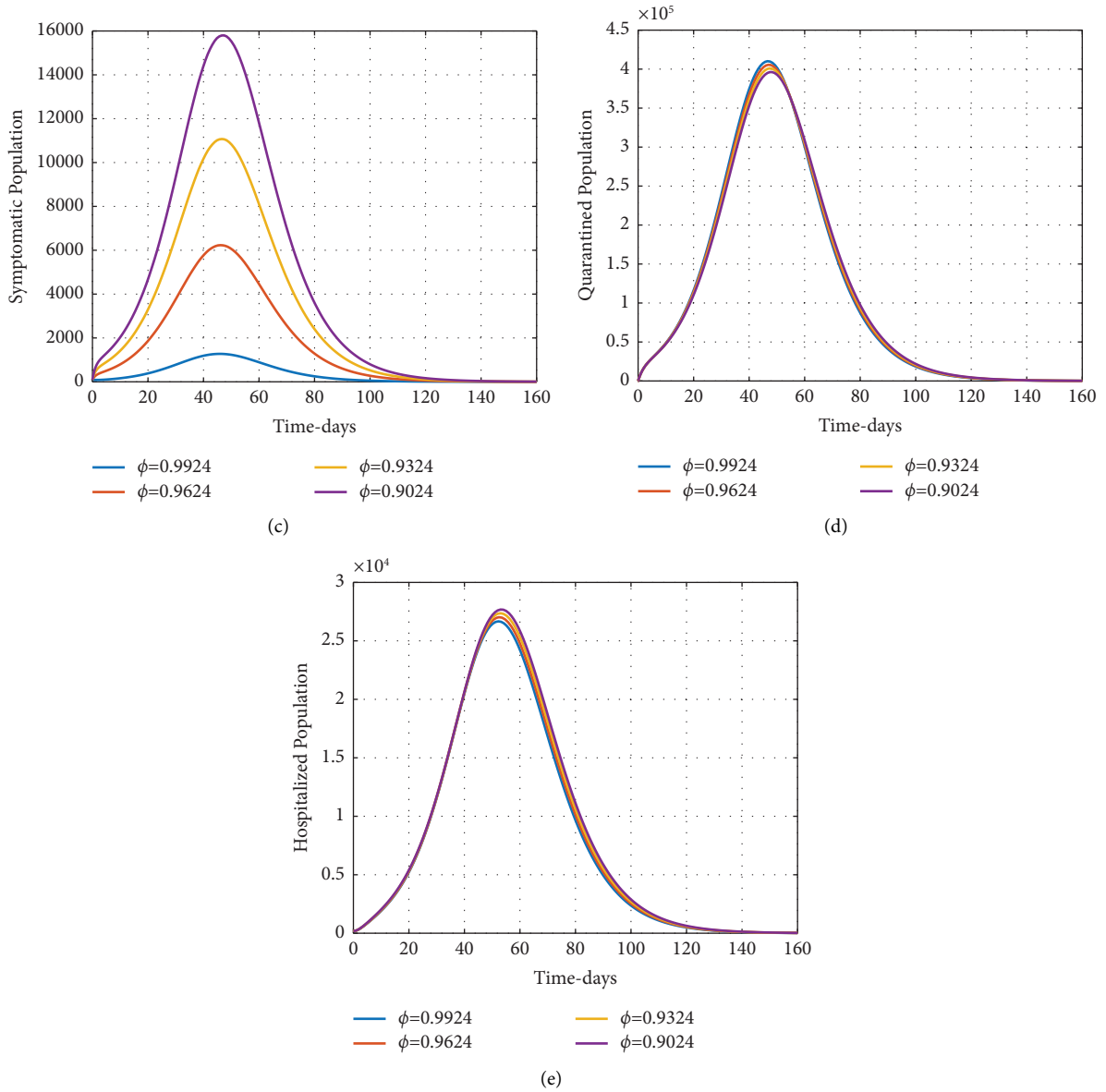


FIGURE 7: The simulation of the infected compartments of system (2) with various values of  $\phi$ . Subgraphs (a)–(e), respectively, represent the behavior of compartments  $E$ ,  $A$ ,  $I$ ,  $Q$ , and  $H$ .

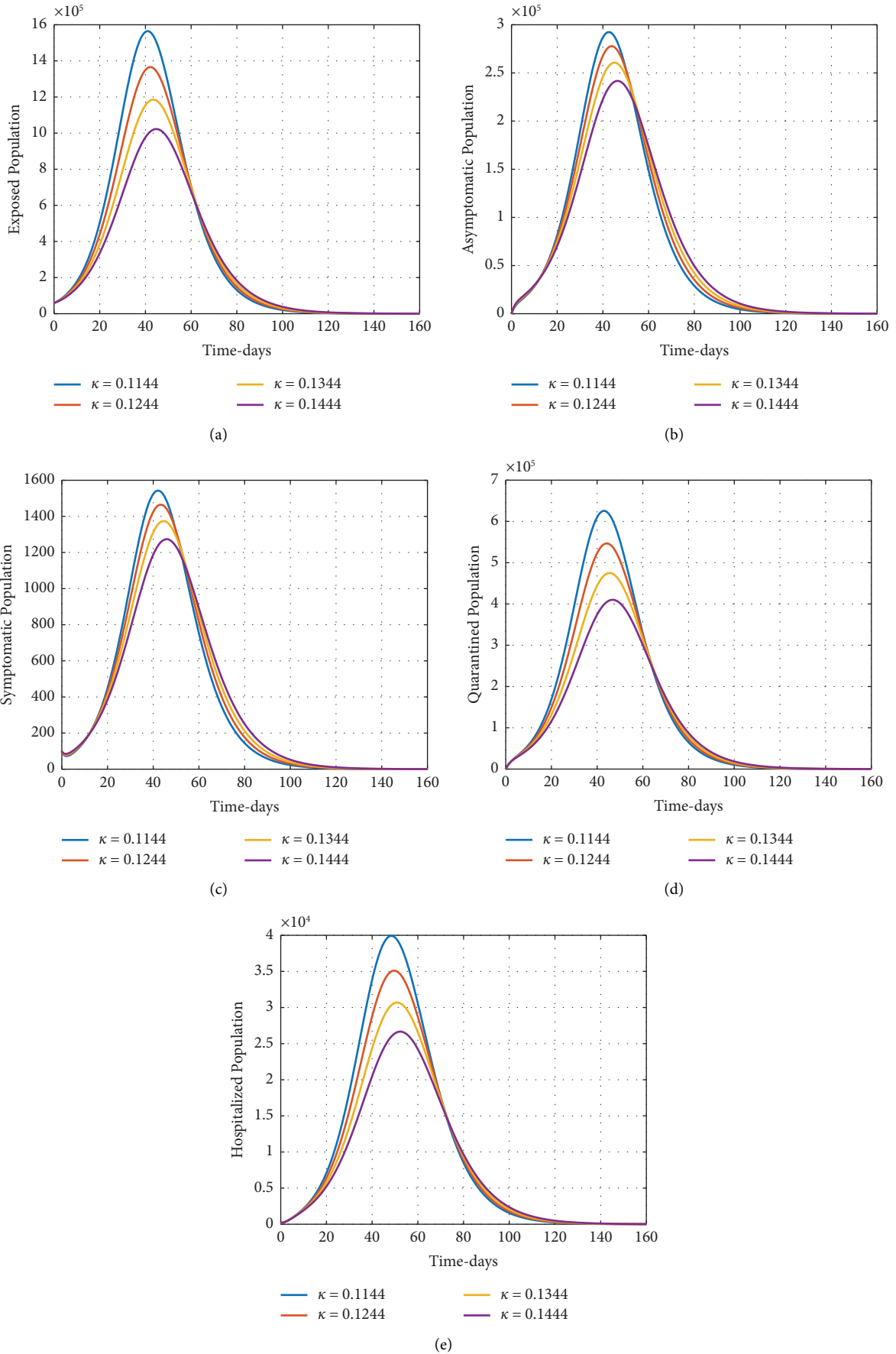


FIGURE 8: The simulation of the infected compartments of system (2) with various values of  $\kappa$ . Subgraphs (a)–(e), respectively, represent the behavior of compartments  $E$ ,  $A$ ,  $I$ ,  $Q$ , and  $H$ .

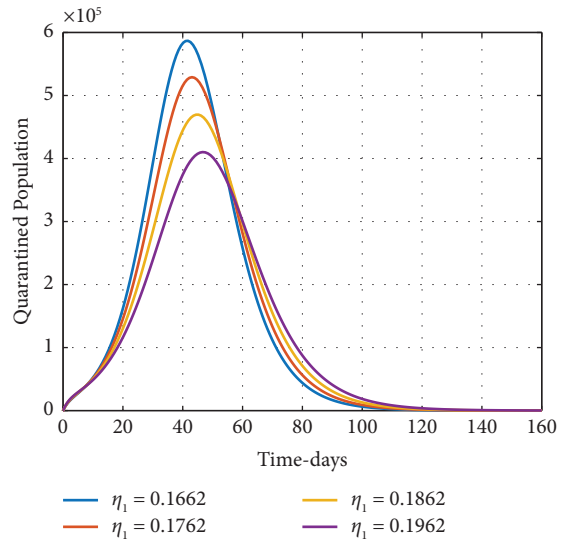
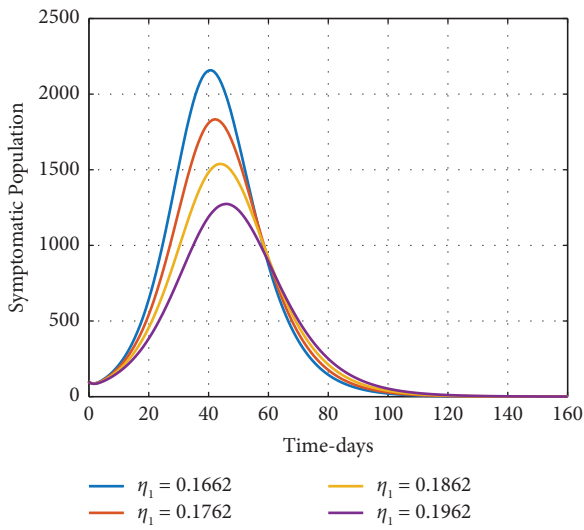
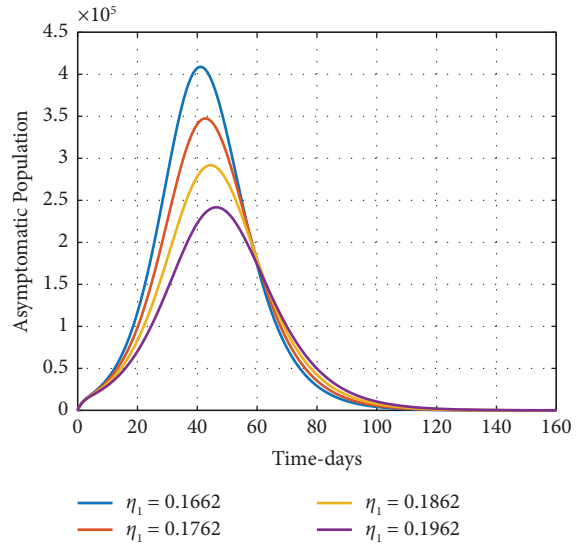
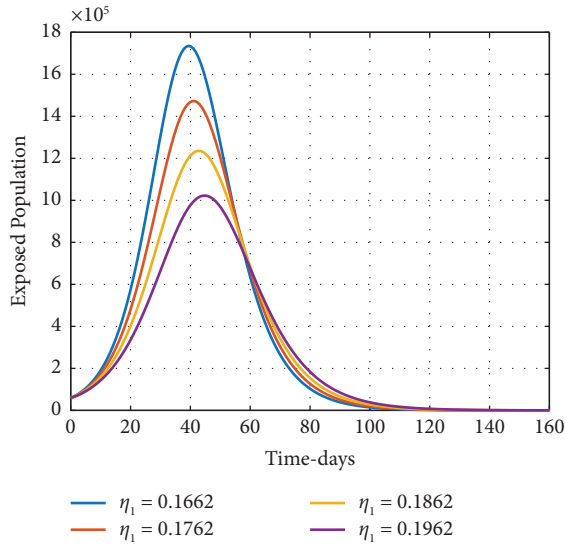


FIGURE 9: Continued.



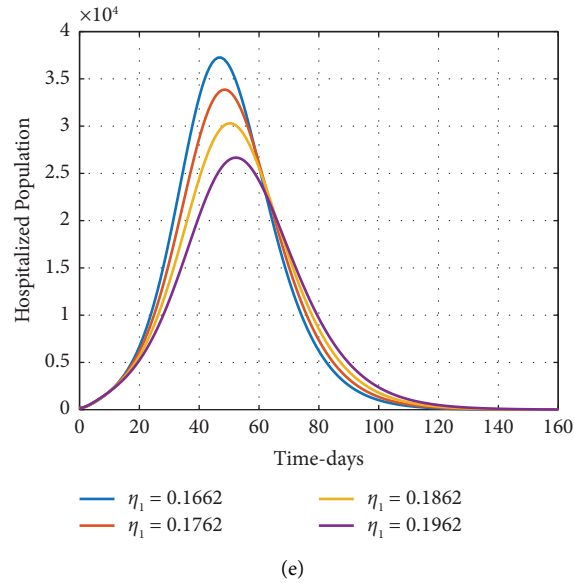


FIGURE 9: The simulation of the infected compartments of system (2) with various values of  $\eta_1$ . Subgraphs (a)–(e), respectively, represent the behavior of compartments  $E$ ,  $A$ ,  $I$ ,  $Q$ , and  $H$ .

In Figure 9, we plotted the role of the quarantine rate of exposed individuals shown by  $\eta_1$ , which shows a significant decrease in the future infected cases in different compartments.

## 6. Conclusion

We formulated and analyzed a new mathematical model for understanding the COVID-19 dynamics with hospitalization and quarantine with the recent data of Saudi Arabia. The real data of the fourth wave which are the recent cases are considered.

We studied the model-related properties in detail. We obtained the equilibrium points of the system. We discussed that the infection-free equilibrium of the model is found to be locally asymptotically stable when the basic reproduction number  $\mathcal{R}_0 < 1$ . We studied the global asymptotical stability of the model at the infection-free state and found it globally asymptotically stable for  $\mathcal{R}_0 \leq 1$ . The global asymptotical stability of the model ensures the impossibilities of the backward bifurcation in the present COVID-19 infection model. Also, the endemic expressions indicate that there is no possible occurrence of the backward bifurcation for the proposed model. The possibility of the backward bifurcation would lead to that the infection will lost in the community and hence endemic.

In light of the COVID-19 cases that have been reported in Saudi Arabia, we used the least square curve fitting techniques to parameterize the model. We considered some of the parameters from the literature and have cited them in Table 1. The rest of the parameters are fitted to the infected cases in Saudi Arabia. The realistic parameter values obtained through the data fitting have been used to estimate the basic reproduction number  $\mathcal{R}_0 \approx 1.2988$ . The parameters impact on the model has been shown graphically, and it can be seen that the

infection can be minimized well if the number of individuals identified exposed to the virus could be quarantined early. This early quarantine of the exposed individuals will minimize the future cases of the virus in the country. We observed that quarantine and hospitalization are both effective for the eradication of the disease. The impact of the parameters and the model's infected compartments has been simulated and we found that the variation in these contacts/parameters rarely reduce the disease future cases significantly. It has been concluded from the results that exposed, asymptomatic, hospitalized, and symptomatic individuals' interaction with healthy individuals increased the future cases of infection. It is better to minimize such contact with healthy individuals to reduce the future risk and increase of the infection. The simulation results indicate that we may certainly decrease the number of infected cases by following the suggestions of the WHO well; as shown in a mathematical model, the contacts such as  $(\xi_1, \dots, \xi_4)$  must be minimized. For COVID-19, quarantine and hospitalization are important in order to control the possible spread of the disease, so in this work, we used both quarantine and hospitalization and also the asymptomatic class, which can be used for any country data to get the result accurately. This model contains all the possible routes of the disease transmission that take place in COVID-19, so it is a perfect model.

## Data Availability

The data used to support the findings of this study are available from the corresponding author upon reasonable request.

## Conflicts of Interest

The authors declare that they have no conflicts of interest.

## Acknowledgments

The Deanship of Scientific Research (DSR) at King Abdulaziz University (KAU), Jeddah, Saudi Arabia, has funded this Project under grant no. (G: 154-130-1443). Open access funding was enabled and organized by SANLiC Gold.

## References

- [1] K. J. James, "Global economic effects of covid-19," Technical report, Congressional Research Service, Washington, DC, USA, 2021.
- [2] Us Global Leadership Coalition, "Covid-19 brief: impact on the economies of low-income countries," 2021, <https://www.usgic.org/coronavirus/economies-of-developing-countries/>.
- [3] D. Havrlant, A. Darandary, and A. Muhsen, "Early estimates of the impact of the covid-19 pandemic on gdp: a case study of Saudi Arabia," *Applied Economics*, vol. 53, no. 12, pp. 1317–1325, 2021.
- [4] Saudi arabia, "Coronavirus cases," <https://www.worldometers.info/coronavirus/country/saudi-arabia/>.
- [5] Q. Zeng, B. Bie, Q. Guo et al., "Hyperpolarized xe nmr signal advancement by metal-organic framework entrapment in aqueous solution," *Proceedings of the National Academy of Sciences*, vol. 117, no. 30, pp. 17558–17563, 2020.
- [6] H.-Y. Jin and Z.-A. Wang, "Global stabilization of the full attraction-repulsion keller-segel system," *Discrete & Continuous Dynamical Systems- A*, vol. 40, no. 6, pp. 3509–3527, 2020.
- [7] W. Lyu and Z.-A. Wang, "Logistic damping effect in chemotaxis models with density-suppressed motility," *Advances in Nonlinear Analysis*, vol. 12, no. 1, pp. 336–355, 2022.
- [8] H.-Y. Jin and Z.-A. Wang, "Asymptotic dynamics of the one-dimensional attraction–repulsion keller–segel model," *Mathematical Methods in the Applied Sciences*, vol. 38, no. 3, pp. 444–457, 2015.
- [9] X. Xie, X. Jin, G. Wei, and C.-T. Chang, "Monitoring and early warning of smes' shutdown risk under the impact of global pandemic shock," *Systems*, vol. 11, no. 5, p. 260, 2023.
- [10] Z. Guan, J. Jing, X. Deng et al., "Deepmih: deep invertible network for multiple image hiding," *IEEE Transactions on Pattern Analysis and Machine Intelligence*, vol. 45, no. 1, pp. 372–390, 2023.
- [11] Y. Wang, Y. Su, W. Li, J. Xiao, X. Li, and A.-A. Liu, "Dual-path rare content enhancement network for image and text matching," *IEEE Transactions on Circuits and Systems for Video Technology*, vol. 33, no. 10, pp. 6144–6158, 2023.
- [12] W. Li, Y. Wang, Y. Su, X. Li, A. Liu, and Y. Zhang, "Multi-scale fine-grained alignments for image and sentence matching," *IEEE Transactions on Multimedia*, vol. 25, pp. 543–556, 2023.
- [13] T. Li, T. Xia, H. Wang et al., "Smartphone app usage analysis: datasets, methods, and applications," *IEEE Communications Surveys & Tutorials*, vol. 24, no. 2, pp. 937–966, 2022.
- [14] A. Atangana, "Modelling the spread of covid-19 with new fractal-fractional operators: can the lockdown save mankind before vaccination?" *Chaos, Solitons & Fractals*, vol. 136, Article ID 109860, 2020.
- [15] Z. Xu, H. Zhang, and Z. Huang, "A continuous markov-chain model for the simulation of covid-19 epidemic dynamics," *Biology*, vol. 11, no. 2, p. 190, 2022.
- [16] A. Muniyappan, B. Sundarappan, P. Manoharan et al., "Stability and numerical solutions of second wave mathematical modeling on covid-19 and omicron outbreak strategy of pandemic: analytical and error analysis of approximate series solutions by using hpm," *Mathematics*, vol. 10, no. 3, p. 343, 2022.
- [17] M. H. DarAssi, M. A. Safi, M. A. Khan, A. Beigi, A. A. Aly, and M. Y. Alshahrani, "A mathematical model for sars-cov-2 in variable-order fractional derivative," *The European Physical Journal- Special Topics*, vol. 231, pp. 1905–1914, 2022.
- [18] M. Pitchaimani and A. Saranya Devi, "Fractional dynamical probes in covid-19 model with control interventions: a comparative assessment of eight most affected countries," *The European Physical Journal Plus*, vol. 137, no. 3, pp. 370–437, 2022.
- [19] H. Habenom, M. Aychluh, D. L. Suthar, Q. Al-Mdallal, and S. D. Purohit, "Modeling and analysis on the transmission of covid-19 pandemic in Ethiopia," *Alexandria Engineering Journal*, vol. 61, no. 7, pp. 5323–5342, 2022.
- [20] J. N. Paul, S. S. Mirau, and I. S. Mbalawata, "Mathematical approach to investigate stress due to control measures to curb covid-19," *Computational and Mathematical Methods in Medicine*, vol. 2022, Article ID 7772263, 23 pages, 2022.
- [21] H. M. Youssef, N. Alghamdi, M. A. Ezzat, A. A. El-Bary, and A. M. Shawky, "A proposed modified seiqr epidemic model to analyze the covid-19 spreading in Saudi Arabia," *Alexandria Engineering Journal*, vol. 61, no. 3, pp. 2456–2470, 2022.
- [22] N. Anggriani and L. K. Beay, "Modeling of COVID-19 spread with self-isolation at home and hospitalized classes," *Results in Physics*, vol. 36, Article ID 105378, 2022.
- [23] Y.-M. Chu, A. Ali, M. A. Khan, S. Islam, and S. Ullah, "Dynamics of fractional order covid-19 model with a case study of Saudi Arabia," *Results in Physics*, vol. 21, Article ID 103787, 2021.
- [24] S. Bhattar, S. Bhattar, K. Jangid, A. Abidemi, K. Owolabi, and S. Purohit, "A new fractional mathematical model to study the impact of vaccination on covid-19 outbreaks," *Decision Analytics Journal*, vol. 6, Article ID 100156, 2023.
- [25] A. M. Mishra, S. D. Purohit, K. M. Owolabi, and Y. D. Sharma, "A nonlinear epidemiological model considering asymptotic and quarantine classes for sars cov-2 virus," *Chaos, Solitons & Fractals*, vol. 138, Article ID 109953, 2020.
- [26] M. Aychluh, S. D. Purohit, P. Agarwal, and D. L. Suthar, "Atangana–baleanu derivative-based fractional model of covid-19 dynamics in Ethiopia," *Applied Mathematics in Science and Engineering*, vol. 30, no. 1, pp. 635–660, 2022.
- [27] S. Kumawat, S. Bhattar, D. L. Suthar, S. D. Purohit, and K. Jangid, "Numerical modeling on age-based study of coronavirus transmission," *Applied Mathematics in Science and Engineering*, vol. 30, no. 1, pp. 609–634, 2022.
- [28] I. A. Baba, U. Humphries, and F. A. Rihan, "Role of vaccines in controlling the spread of covid-19: a fractional-order model," *Vaccines*, vol. 11, no. 1, p. 145, 2023.
- [29] S. Kumar, R. Kumar, S. Momani, and S. Hadid, "A study on fractional covid-19 disease model by using hermite wavelets," *Mathematical Methods in the Applied Sciences*, vol. 46, no. 7, pp. 7671–7687, 2023.
- [30] P. Kumar and V. Suat Erturk, "The analysis of a time delay fractional covid-19 model via caputo type fractional derivative," *Mathematical Methods in the Applied Sciences*, vol. 46, no. 7, pp. 7618–7631, 2023.

- [31] M. H. DarAssi, I. Ahmad, M. Z. Meetei, M. Alsulami, M. A. Khan, and E. M. Tag-eldin, "The impact of the face mask on sars-cov-2 disease: mathematical modeling with a case study," *Results in Physics*, vol. 51, Article ID 106699, 2023.
- [32] Q. Li, Y. Miao, X. Zeng, C. S. Tarimo, C. Wu, and J. Wu, "Prevalence and factors for anxiety during the coronavirus disease 2019 (covid-19) epidemic among the teachers in China," *Journal of Affective Disorders*, vol. 277, pp. 153–158, 2020.
- [33] J. Zhang, J. Xie, W. Shi, Y. Huo, Z. Ren, and D. He, "Resonance and bifurcation of fractional quintic mathieu–duffing system," *Chaos*, vol. 33, no. 2, Article ID 23131, 2023.
- [34] S. Liu, B. Yang, Y. Wang, J. Tian, L. Yin, and W. Zheng, "2d/3d multimode medical image registration based on normalized cross-correlation," *Applied Sciences*, vol. 12, no. 6, p. 2828, 2022.
- [35] Y. Zhang, R. Liu, A. A. Heidari et al., "Towards augmented kernel extreme learning models for bankruptcy prediction: algorithmic behavior and comprehensive analysis," *Neuro-computing*, vol. 430, pp. 185–212, 2021.
- [36] Y. Liu, J. Tian, R. Hu et al., "Improved feature point pair purification algorithm based on sift during endoscope image stitching," *Frontiers in Neurorobotics*, vol. 16, Article ID 840594, 2022.
- [37] S. Khajanchi, K. Sarkar, and S. Banerjee, "Modeling the dynamics of covid-19 pandemic with implementation of intervention strategies," *The European Physical Journal Plus*, vol. 137, no. 1, pp. 129–222, 2022.
- [38] N. H. Sweilam, S. M. Al-Mekhlafi, A. Almutairi, and D. Baleanu, "A hybrid fractional covid-19 model with general population mask use: numerical treatments," *Alexandria Engineering Journal*, vol. 60, no. 3, pp. 3219–3232, 2021.
- [39] I. M. Hezam, A. Foul, and A. Alrasheedi, "A dynamic optimal control model for covid-19 and cholera co-infection in Yemen," *Advances in Difference Equations*, vol. 2021, no. 1, pp. 108–130, 2021.
- [40] A. Atangana and S. İğret Araz, "Mathematical model of covid-19 spread in Turkey and South Africa: theory, methods, and applications," *Advances in Difference Equations*, vol. 2020, no. 1, pp. 1–89, 2020.
- [41] N. Anggriani, M. Z. Ndi, R. Amelia, W. Suryaningrat, and M. A. A. Pratama, "A mathematical covid-19 model considering asymptomatic and symptomatic classes with waning immunity," *Alexandria Engineering Journal*, vol. 61, no. 1, pp. 113–124, 2022.
- [42] J. Mishra, R. Agarwal, and A. Atangana, *Mathematical Modeling and Soft Computing in Epidemiology*, CRC Press, Boca Raton, FL, USA, 2020.
- [43] N. Bicudo, E. Bicudo, J. D. Costa, J. A. L. P. Castro, and G. B. Barra, "Co-infection of sars-cov-2 and dengue virus: a clinical challenge," *Brazilian Journal of Infectious Diseases*, vol. 24, no. 5, pp. 452–454, 2020.
- [44] A. Viguier, A. Veneziani, G. Lorenzo et al., "Diffusion–reaction compartmental models formulated in a continuum mechanics framework: application to covid-19, mathematical analysis, and numerical study," *Computational Mechanics*, vol. 66, no. 5, pp. 1131–1152, 2020.
- [45] F. Yang and Z. Zhang, "A time-delay covid-19 propagation model considering supply chain transmission and hierarchical quarantine rate," *Advances in Difference Equations*, vol. 2021, no. 1, pp. 191–221, 2021.
- [46] A. Raza, M. Rafiq, J. Awrejcewicz, N. Ahmed, and M. Mohsin, "Dynamical analysis of coronavirus disease with crowding effect, and vaccination: a study of third strain," *Nonlinear Dynamics*, vol. 107, no. 4, pp. 3963–3982, 2022.
- [47] N. Ahmed, A. Elsonbaty, A. Raza, M. Rafiq, and W. Adel, "Numerical simulation and stability analysis of a novel reaction–diffusion covid-19 model," *Nonlinear Dynamics*, vol. 106, no. 2, pp. 1293–1310, 2021.
- [48] A. Raza, J. Awrejcewicz, M. Rafiq, and M. Mohsin, "Break-down of a nonlinear stochastic nipah virus epidemic models through efficient numerical methods," *Entropy*, vol. 23, no. 12, p. 1588, 2021.
- [49] A. Raza, M. S. Arif, and M. Rafiq, "A reliable numerical analysis for stochastic gonorrhoea epidemic model with treatment effect," *International Journal of Biomathematics*, vol. 12, no. 6, Article ID 1950072, 2019.
- [50] H. Hamam, A. Raza, M. M. Alqarni et al., "Stochastic modelling of lassa fever epidemic disease," *Mathematics*, vol. 10, no. 16, p. 2919, 2022.
- [51] A. Raza, J. Awrejcewicz, M. Rafiq, N. Ahmed, and M. Mohsin, "Stochastic analysis of nonlinear cancer disease model through virotherapy and computational methods," *Mathematics*, vol. 10, no. 3, p. 368, 2022.
- [52] A. Rajput, M. Sajid, S. Chandra, and R. Aggarwal, "Optimal control strategies on covid-19 infection to bolster the efficacy of vaccination in India," *Scientific Reports*, vol. 11, no. 1, pp. 1–18, 2021.
- [53] T. Aggarwal, A. Rajput, and M. Sajid, "Modeling the optimal interventions to curtail the cluster based covid-19 pandemic in India: efficacy of prevention measures," *Applied and Computational Mathematics*, vol. 20, pp. 70–94, 2021.
- [54] E. Boro and B. Stoll, "Barriers to COVID-19 health products in low-and middle-income countries during the COVID-19 pandemic: a rapid systematic review and evidence synthesis," *Frontiers in Public Health*, vol. 10, Article ID 928065, 2022.
- [55] S. Li and Y. Shan, "Latest research advances on novel coronavirus pneumonia," 2020, <https://pesquisa.bvsalud.org/global-literature-on-novel-coronavirus-2019-ncov/resource/pt/ppcovidwho-4385>.
- [56] Y. Chen, A. H. Wang, B. Yi et al., "Epidemiological characteristics of infection in covid-19 close contacts in ningbo city," *Zhonghua liu xing bing xue za zhi= Zhonghua liuxingbingxue zazhi*, vol. 41, no. 5, pp. 667–671, 2020.
- [57] PRC Legal Provisions, "Heilongjiang provincial health committee," <http://wsjkw.hlj.gov.cn/>.
- [58] C. Xiong, "A detailed explanation of survival time for covid-19 virus in the environment," *China Food Safety Magazine*, vol. 5, no. 22–25, 2020.
- [59] Middle East & Africa, "Strong immune response found in asymptomatic patients; virus crosses throat membrane into brain," <https://www.reuters.com/article/health-coronavirus-science-int--iduskbn28a2t5>.
- [60] R. J. Boyton and D. M. Altmann, "The immunology of asymptomatic sars-cov-2 infection: what are the key questions?" *Nature Reviews Immunology*, vol. 21, no. 12, pp. 762–768, 2021.
- [61] D. Yetman, "What to know about asymptomatic covid-19," <https://www.healthline.com/health/what-is-asymptomatic-covid>.
- [62] P. Van den Driessche and J. Watmough, "Reproduction numbers and sub-threshold endemic equilibria for compartmental models of disease transmission," *Mathematical Biosciences*, vol. 180, no. 1–2, pp. 29–48, 2002.

- [63] A. B. Gumel, E. A. Iboi, C. N. Ngonghala, and E. H. Elbasha, “A primer on using mathematics to understand covid-19 dynamics: modeling, analysis and simulations,” *Infectious Disease Modelling*, vol. 6, pp. 148–168, 2021.
- [64] E. A. Iboi, C. N. Ngonghala, and A. B. Gumel, “Will an imperfect vaccine curtail the covid-19 pandemic in the us?” *Infectious Disease Modelling*, vol. 5, pp. 510–524, 2020.
- [65] A. Green, “A tribute to some of the doctors who died from covid-19,” *The Lancet*, vol. 396, no. 10264, pp. 1720–1729, 2020.
- [66] World Health Organization, “The impact of covid-19 on health and care workers: a closer look at deaths,” Technical report, World Health Organization, Geneva, Switzerland, 2021.
- [67] M. Zhan, Y. Qin, X. Xue, and S. Zhu, “Death from covid-19 of 23 health care workers in China,” *New England Journal of Medicine*, vol. 382, no. 23, pp. 2267–2268, 2020.